IEEE Access
Multidisciplinary | Rapid Review | Open Access Journal

Optimal Borehole Energy Storage Charging Strategy in a Low Carbon Space Heat System

Wei Wei[1], Chenghong Gu[1], Da Huo[1], Simon LeBlond[1,2], and Xiaohe Yan[1]

[1]*Dept. of Electronic and Electrical Eng., University of Bath, Bath, BA2 7AY, UK*
[2]*Swanbarton, Wiltshire, SN16 0NX, UK*

ABSTRACT Domestic heating is the major demand of energy systems, which can bring significant uncertainties to system operation and shrink the security margin. From this aspect, the borehole system, as a interseasonal heating storage, can effectively utilize renewable energy to provide heating to ease the adverse impact from domestic heating. This paper proposes an optimal charging strategy for borehole thermal storage by harvesting energy from PV generation in a low carbon space heating system. The system optimizes the heat injection generated by Air Source Heat Pump in the charging seasons to charge the borehole, which provides high inlet temperature for Ground Source Heat Pump to meet space heating demand in discharging seasons. The borehole is modelled by Partial Differential Equations (PDEs), solved by the Finite Element method at both 2D and 3D for volume simulation. The Pattern Search Optimization is used to resolve the model. The case study illustrates that with the optimal charging strategies, less heat flux injection can help the borehole to reach a higher temperature so that the heating system is more efficient compared to boilers. This work can benefit communities with seasonable borehole storage to provide clean but low-cost heating and also maximize PV penetration.

INDEX TERMS Inter-seasonal borehole thermal energy storage (BTES), Air source heat pump (ASHP), Ground source heat pump (GSHP), Optimal charging strategy, Photovoltaic (PV).

I. INTRODUCTION

The massive utilization of fossil energy has resulted in air pollution and global warming [1, 2]. In order to reduce the damage, renewable energy and other environmentally friendly technologies have been widely introduced worldwide. According to the Department of Environment and Climate Change (UK), around 30% of energy consumption is in the domestic sector, responsible for 38% of greenhouse gas emissions [3]. Further, within domestic energy consumption, there are mainly four major energy appliances: Cooking (3%); Lighting and appliances (18%); Water (18%); and Space heating (61%) [4]. It is clear that space heating is the largest energy demand and thus it is important to decarbonize the space heating system by using low-carbon technologies. However, it is very challenging to reduce the energy consumption in space heating [4, 5], as it fairly complicated affected by the behaviours of occupants, the heating systems, house types, and other societal factors [6]. Many efforts have been dedicated to increasing the efficiency of heating energy, such as cavity wall insulation, but they do not always effectively save energy [7].

Heat pumps are more convenient to operate and have better opportunities to reduce carbon emissions by providing efficient heating [8]. In heat pumps, electricity drives a refrigerant cycle to move heat from a low-temperature source to a high-temperature sink. Electric heat pumps are forecasted to be able to reduce CO_2 emissions by more than 90% by 2050 [9]. It is assessed that the air source heat pump (ASHP) could reduce 12% CO_2 emission compared to gas boilers, but the operation cost might increase by 10% decided by operation parameters [8]. Compared to ASHP, ground source heat pump (GSHP) always has a steady heat source, as the ground temperature is much higher and more stable than the ambient air temperature. However, the installation of GSHP is very complicated.

The borehole thermal energy storage (BTES) is a ground-based heat storage with longer asset lifetime compared to other energy storage. In BTES, there are four components – borehole, backfilling material (grout), U-shaped tube and the fluid, which will be explained in the later section. The borehole array is buried deep underground, requiring less maintenance and minimal heat replenishment. The flowing fluid in the borehole pipe is water with mono-ethylene glycol and the glycol prevents the fluid freezing until the temperature reaches -15 °C so that it is suitable for operating along with heat pumps. BTES allows the heating system to store heat and use it later more efficiently. The charged borehole has less heat loss to the surrounding mass because of the steady temperature and good insulating properties of the ground.

The modelling of borehole field response can be realized in several ways. In the early studies of borehole heat energy storage, the analysis of the heat transfer of borehole is challenging due to the transient heat transfer between the media and surrounding geometry [10]. Some studies have been dedicated to this topic mainly by using analytical approaches [11-16] and numerical methods [17-20]. The main difference between the two methods is in the treatment of temperature distribution. In analytical models, the borehole internal region is neglected and the heat transfer is mainly between the borehole wall and surrounding soil. By contrast, numerical models solve the temperature across the whole borehole region [21]. From the past years of studies on borehole storage, there are three main objectives based on the analytical and numerical methods, determining borehole size, quantifying borehole thermal performance, and validating the borehole model.

There are several papers investigating Finite Element numerical simulation for borehole study, such as [22, 23]. Authors verify the borehole model and simulate the long-time heat transfer process with constant heat inputs. In [22], the authors explain the difference between the middle point temperature and the borehole wall temperature. In [23], the authors compare the single borehole and group borehole area temperatures. A more thorough research on borehole operation was carried out in [24]. In [24], the authors consider heating and cooling under different weather conditions with temperature as a constraint, but borehole arrays geometry layout is ignored. To summarize, the current work on borehole modelling lacks thorough focus on the long-term borehole wall temperature behaviour response under different heat injections and extractions. The borehole modelling involves borehole geography layout and optimizing the borehole storage process within a whole heating system. However, most borehole modelling is conducted in an isolated manner, without integrating it into a local heating system and exploring the charging.

This paper proposes a novel local heating system by combining photovoltaic (PV), heat pumps and seasonal borehole heating storage. This work is a part of a practical borehole heating project demonstrated in Bristol UK [8]. The system allows PV energy to charge the borehole with high-temperature fluid via ASHP, providing high evaporate inlet temperature for heat pumps during the discharging season. This paper mainly focuses on the borehole wall temperature and the efficiency of heat pumps during the charging season. Numerical borehole modelling is developed to generate accurate temperature profiles. According to the geography layout, a group of boreholes are displayed in a certain area using Partial Differential Equations (PDEs). The Finite Element method is used to solve the PDEs in different dimensions, 2D for cross section simulation and 3D for volume simulation. The Pattern Search Optimization is used for the charging to enable better heat pump performance. With the optimal operation, borehole heat storage and heat pumps can cooperate efficiently to store heat for discharging the season.

The main contribution of the paper is: i) it designs a more efficient method to charge the borehole via using renewable energy to reduce total energy demand and CO_2 emissions; ii) it studies the impact of temperature and borehole geometry on charging efficiency; iii) it develops an optimization model to provide heat pumps with a high-temperature environment; iv) it extensively compares different indexes to measure the effectiveness of three charging strategies.

The remainder of the paper is organized as follows: Section II, an overview of the heating system is presented. Section III, a borehole model is built to provide the temperature data and the heat pump model is built to study the efficiency. In Section IV, the optimization method is introduced followed by Section V with system input and the case study with results comparison. In Section VI, conclusions are drawn.

II. OVERVIEW OF THE LOW CARBON HEATING SYSTEM

Combined with heat pumps, the inter-seasonal borehole heat storage can be efficiently operated to gain maximum benefits. The main components of this low carbon heating systems include a) PV panels providing electricity to heat pumps, b) heat pumps generating heat flux, and c) borehole storing heat energy. Figs. 1 and 2 illustrate the system working mechanism in charging and discharging seasons.

In the summer charging season, the temperature is high and thus there is no space heating demand. Fig. 1 is the process of borehole active charging during the summer time. The PV installed along the borehole generates electricity to support the Air Source Heat Pump (ASHP), which produces heat without incurring extra costs of electricity consumption. The generated heat will be stored in the borehole to increase the base temperature of the ground.

In the winter discharging season as shown in Fig. 2, it is too cold to operate ASHP due to low ambient air temperature but the GSHP with relatively steady heat source can supply

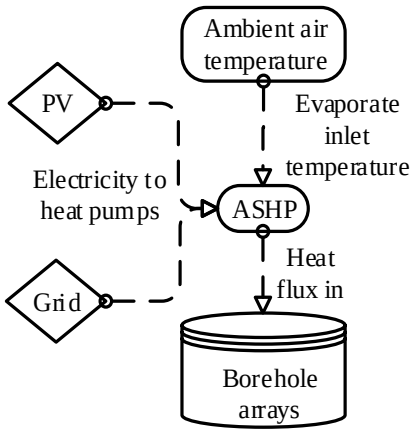

FIGURE. 1 The charging process of the heating system (in summer)

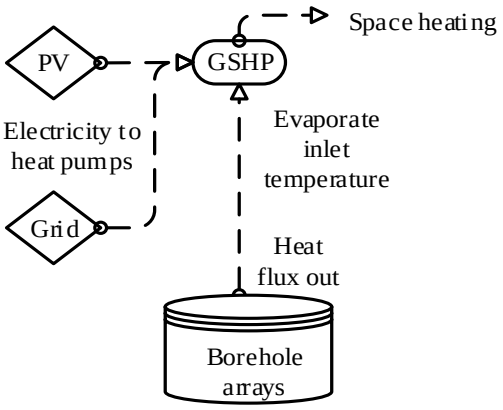

FIGURE. 2 The charging process of the heating system (in winter)

the heat demand. The hot water stored in the borehole during the summer is the heat source, providing GSHP with a higher input temperature. With higher inlet temperature, GSHP has batter performance to provide space heating. Because of the low PV generation during the winter, the grid electricity will provide the extra demanded electricity for the GSHP.

III. SYSTEM MODELLING

A. BOREHOLE MODELLING

This paper uses the Finite Element model, which can accurately reflect borehole temperature map, to calculate heat transfer in the whole area. For a single borehole in Fig. 3 (a), the U-shaped pipe can be simplified to a single cylinder pipe [10] and the cross-section view is in Fig. 3(b). The fluid area represents the combined area of the U-shaped tube placed in the middle of the borehole. According to the different heat flux along the simulated time, the temperature of all nodes is exported as a matrix and the nodes representing the borehole wall will be selected for further calculation. The grout in Fig. 3(b) represents the backfilling material in Fig. 3(a). Fig. 3(c) is the total 12-borehole layout. In the model, the edges are set as Neumann boundary with heat flux/temperature information and the subsections are set as the Dirichlet boundary.

The temperature used in the system is the borehole wall temperature instead of fluid temperature. The pipe carries high-temperature fluid varying dramatically and the heat energy settles in the borehole wall and its surrounding area. When the borehole needs to discharge, the heat already settles in the borehole and the fluid extracts heat from the borehole wall and surrounding area. Fig. 4 details the system flowchart of calculating the borehole temperature across the whole storage area starting with modelling set up and the

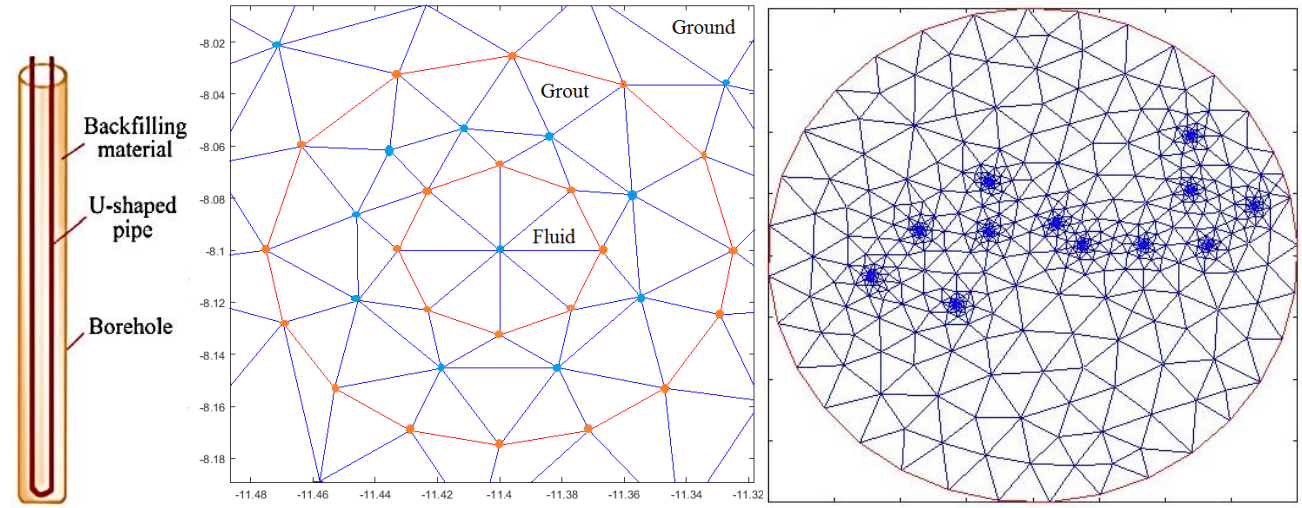

(a) The single borehole [1] (b) Cross-section view of a single borehole (c) 12-borehole geometry layout of the system

FIGURE. 3 The layout and geometry of boreholes

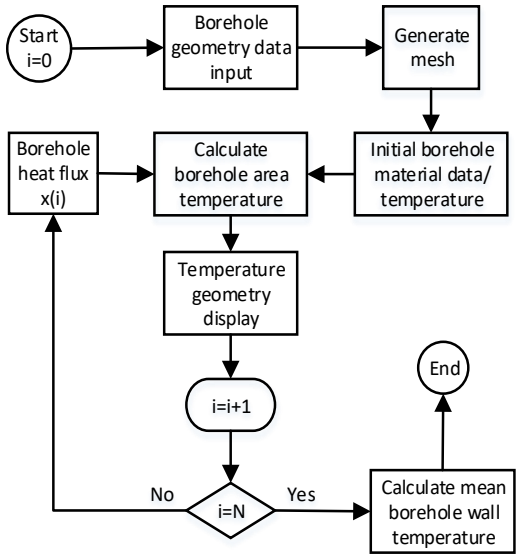

FIGURE. 4 The flowchart for borehole temperature modelling

initial conditions of the borehole material and surrounding ground. With all the input information, borehole model calculates the temperature step by step. The flowchart Fig. 4 can be realized with the following two fundamental steps:

1) GEOMETRY AND COEFFICIENTS SETTING

Boundaries, edges and subdomains can be created by circle, polygon, rectangle and ellipse objectives, which separate the regions of different materials as shown in Fig. 3.

Once the boundaries, edges, and subdomains are defined, the boundary conditions and PDE specifications are set.

The boundary conditions used in this borehole model are:

Neumann:

$$n \times k \times grad(U) + q \times U = g \tag{1}$$

Dirichlet:

$$h \times U = r \tag{2}$$

Where, k is the coefficient of heat conduction, g is the heat flux, q is the heat transfer coefficient, n, h and r are the function of space, and U is the temperature solution.

In PDE for the heat transfer, the *Parabolic* equation is used.

Parabolic:

$$d\frac{\partial U}{\partial t} - \nabla \cdot (c\nabla U) + aU = f \tag{3}$$

Where, U is the temperature solution in the form of matrix. Temperature solution U is a matrix of N -*by*-T, N is the temperature calculation of each node in the mesh in PDE and T is the number of time steps. a, c, d, f are the scalar PDE coefficients. The coefficients define each node in the mesh during the heat transfer process.

2) GENERATING MESH

Fig. 3 (b) is one of the parallel-connected 12 boreholes in this system. The mesh represents the materials used in the

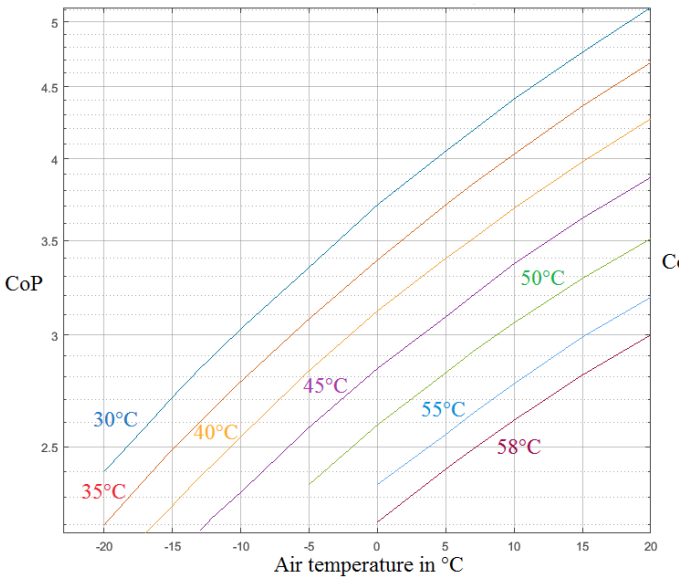

FIGURE. 5 ASHP CoP in different outlet temperature categories

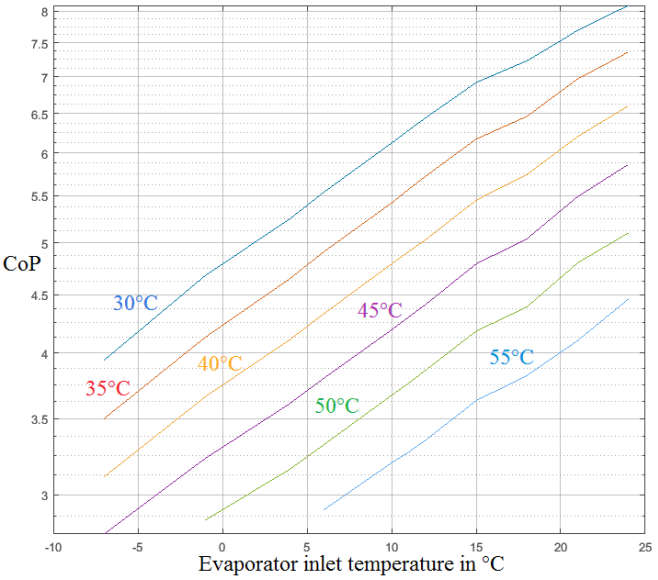

FIGURE. 6 GSHP CoP in different outlet temperature categories

TABLE I
ASHP/GSHP COP PARAMETERS

Condenser outlet temperature		30°C	35°C	40°C	45°C	50°C	55°C	58°C
ASHP	A	0.068	0.062	0.057	0.051	0.047	0.042	0.039
	B	3.7	3.4	3.1	2.8	2.5	2.3	2.2
GSHP	A	0.136	0.126	0.113	0.100	0.091	0.085	---
	B	4.8	4.2	3.7	3.3	2.8	2.4	---

borehole as shown in Fig. 3 (a). The number of triangles affects the simulation time and each node in the mesh represents the temperature point, where all points form the temperature solution matrix.

B. HEAT PUMP MODEL

The ASHP and GSHP are the major low carbon technologies for meeting heating demand in this proposed space heating system. The heap pump data is from the demonstration project in Bristol. From Figs. 5 and 6, for the temperature of each heat pump outlet condenser labelled beside each line within a certain temperature range, the Coefficient of Performance (CoP) can be assumed to be a linear function of the heat pump inlet temperature. The condenser outlet temperature is treated as the heat pump output temperature. With the selected heat pump output temperature, the CoP of the heat pump depends on the heat pump inlet temperature. In general, higher condenser outlet temperature results in lower CoP category, shown in both figures. Within each condenser outlet temperature category, the CoP increases when the evaporate inlet temperature rises.

In this paper, the heat pump inlet temperature is within the linear range so that the CoP value is fitted by

$$CoP_t = A \times T + B \tag{4}$$

Where, A and B are constants which depend on the heat pump condenser outlet temperature shown in TABLE I. In this paper, the condenser outlet temperature of ASHP and GSHP are chosen at 30 °C and 45 °C respectively [8]. With the chosen parameters A and B, the heat pump CoP value can be calculated. *t* is the chosen outlet temperature, and *T* is the heat pump evaporator inlet temperature (°C).

With increasing evaporator inlet temperature, the CoP value increases as well. However, with higher condenser outlet temperature, CoP is generally lower. Table I provides the parameters used in this paper to calculate the heat pump CoP [8]. Equation (5) models the heat output from the heat pump in terms of its electricity consumption:

$$H = CoP_t \times P \tag{5}$$

Where, H is heat output and P is input electricity for the heat pump.

IV. SYSTEM OPTIMIZATION

Based on the system diagram in Figs. 1 and 2, heat pumps convert electricity into heat in both charging and discharging seasons. An optimization model is designed to obtain the lowest system electricity consumption over the whole charging time so that the system uses minimum energy during the charging season to supply the heat demand in the discharging season.

The optimization is carried out by using Pattern Search. The objective function (6) is to find the minimum total heat flux provided by the ASHP during the charging season which is also the minimum electricity consumption from the ASHP. The constraint in (7b) is the upper and lower boundaries of the variable *x* which is the heat flux value in W/m^3. The heat injected into the borehole is from ASHP and the electricity required by operating ASHP is related to its CoP, decided by the inlet evaporate temperature (ambient air temperature) and outlet condenser temperature. According to the ASHP data, the average maximum ASHP heat flux output is around 4541 W/m^3. In the MATLAB PDE tool, for the transient analysis, the heat flux unit is the heat produced per unit volume per time. In the discharging season, *x* equals the heat demand. During the discharging season, the GSHP is assumed to consume a fixed total amount of electricity ($E_{GSHP\ fixed}$) to cover the space heating demand. The $E_{GSHP\ fixed}$ is obtained from one of the base cases explained in the case study.

$$\text{Obj} = \min \sum_{i=1}^{26} x_{(i)} \tag{6}$$

$$0 = E_{GSHP\ fixed} - \sum_{n=27}^{52} E_{GSHP(n)} \tag{7a}$$

$$\begin{cases} 0 \le x_{(i)} \le 4541,\ i = (1{:}26) \\ x_{(n)} = heating\ load,\ n = (27{:}52) \end{cases} \tag{7b}$$

Where, $E_{GSHP(n)}$ is GSHP electricity consumption at step *n*.

$$x_{(i)} = \frac{1000 \times H_{ASHP(i)}}{24 \times 7 \times N_{borehole} \times V_{borehole}}$$

$$= \frac{1000 \times E_{ASHP(i)} \times (A \cdot T_{air(i)} + B)}{24 \times 7 \times N_{borehole} \times V_{borehole}} \tag{8}$$

Where, $H_{ASHP(i)}$ is ASHP heat generation at time step *i* in kWh, and $T_{air(i)}$ is the ambient air temperature at time step *i*. $E_{ASHP(i)}$ is ASHP electricity consumption in kWh provided by PV or the grid. $N_{borehole}$ is the number of the borehole in the system. $V_{borehole}$ is the volume of every single borehole in Fig. 6(a). GSHP operates under the same concept, but the inlet evaporating temperature is the borehole wall temperature. During the discharging season, the borehole wall temperature can be calculated in the Finite Element borehole model and the GSHP electricity consumption is from (9):

$$E_{GSHP(n)} = \frac{H_{GSHP(n)}}{CoP_{GSHP(n)}} = \frac{x_{(n)}}{A \cdot u_{(n)} + B} \tag{9}$$

Where, $u_{(n)}$ is the selected borehole wall temperature matrix (1 *-by-T)* from the temperature solution matrix *u*. The borehole wall temperature value is the average value of all borehole wall temperature points. $H_{GSHP(i)}$ is GSHP heat output, which is the heat demand in the system.

V. CASE STUDY

A. SYSTEM INPUT

The size of the borehole is as follows: i) 12 x 150 m under the ground; ii) U-Pipe diameter x thickness (mm) 40 x 3.7; iii) the material data is in TABLE II.

TABLE II
BOREHOLE MATERIAL PARAMETERS

	Ground	Fluid	Grout
Density (kg/m^3)	2770	1052	1550
Heat capacity (j/(kg.K))	829	3795	1000
Thermal conductivity (W/(m.K))	2.61	0.5	2.1

Due to the enormous mesh size of the borehole, simulation is very time-consuming. As a result, the mesh of the borehole is not refined and the time step is set at one week, which means the borehole is constantly injecting heat during each step. The charging season only involving PV electricity would have more heat loss when the borehole is not charging making the reality worse. The GSHP provides the space heating so that the condenser outlet temperature is set at 45°C in Table I.

One of the most important components in the heating system is the PV panels. The electricity generated from the PV provides low-carbon electricity to the borehole system. The PV weekly generation data and sun radiation data are from the "Photovoltaic Geographical Information System" (PVGIS) [25]. The PV electricity generation used is in the blue line in Fig. 7(a). It is assumed that the surplus PV electricity is exported to the grid with a flat Feed-In-Tariff (FIT) rate of £0.12/kWh. During the summertime, PV generates more electricity compared to the winter time. Grid electricity will be used when the PV electricity output cannot meet the electricity demand of the heat pumps. The heat load and the grid electricity price are from the historical data in [4, 26]. The purple line in Fig 7(a) is the space heat demand which is provided by the GSHP only during discharging season (from week 27 to week 52). The heat demand varies from week to week. Fig. 7(b) shows the weekly electricity price from the historical data [26]. In this system, the maximum available heat output of ASHP is 4,541 W/m^3 and the heat pump information is from [8].

B. CASE SETUP

The system is based on a practical project which provides space heating to a community building and some houses. The case study is designed to study the benefits of different operation of the proposed system between no active charging, with active charging, and with optimized active charging. The impact of heat accumulating in the borehole storage is illustrated. Due to the enormous mesh of the

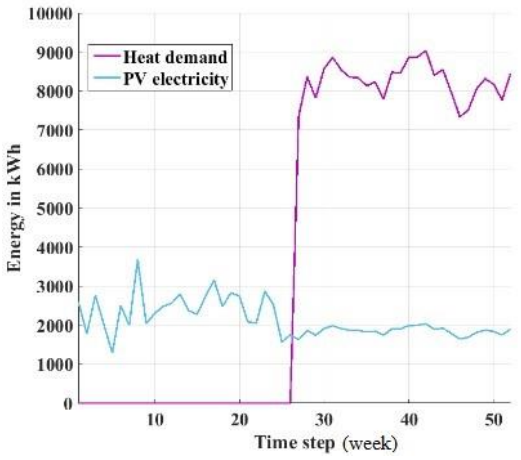

(a) Heat demand and PV electricity generation during the simulation time window [25,26]

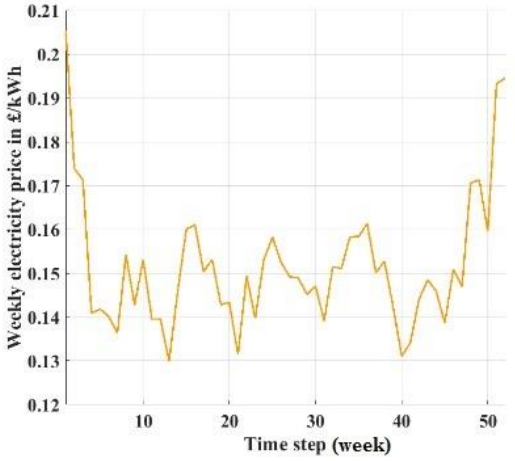

(b) Weekly grid electricity price during the simulation time window[26]

FIGURE. 7 Weekly PV generation, heat demand and electricity price

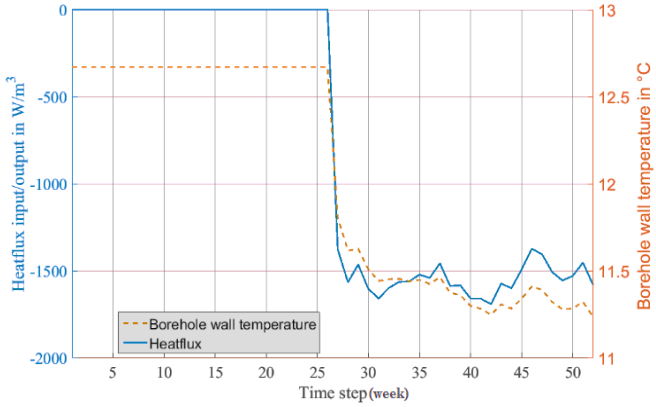

FIGURE. 8 Case 1 borehole wall temperature response to heat flux

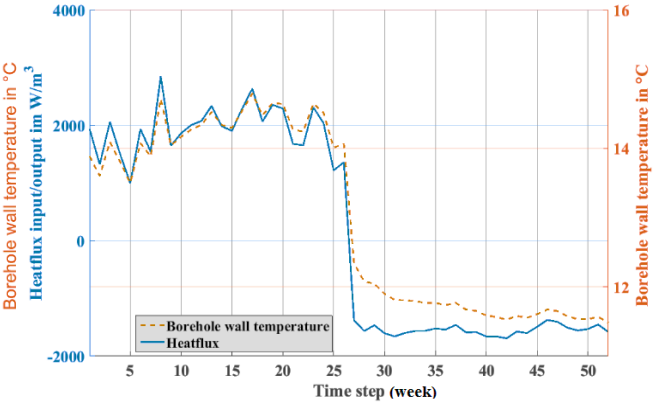

FIGURE. 9 Case 2 borehole wall temperature response to heat flux

borehole model which dramatically affects the optimization time, one week is set as the time step for the simulation. Three cases are here to validate and demonstrate the proposed models: Case 1- without active charging in charging season; Case 2- with active charging according to PV generation; and Case 3- with optimized charging strategy.

1) CASE 1 WITHOUT ACTIVE CHARGING IN CHARGING SEASON

This is the base case, where the borehole is installed to provide the space heating all through the discharging season (heating season) from September to March. In the charging season from April to August, there is no active charging to the borehole, which means the borehole only extracts heat during the discharging season by using the surrounding ground (bedrock) as a heat source. The borehole starting temperature is the same as that of the ground 12.67°C.

In Fig. 8, the solid line represents the heat flux injection/exportation in each time step. The dotted line is the borehole wall temperature responding to the heat flux. Without active charging during the charging season, the borehole temperature remains the same as the ground temperature. When the discharging season ends, the borehole temperature drops from ground temperature to 11.3 °C.

2) CASE 2 WITH ACTIVE CHARGING ACCORDING TO PV GENERATION

In this case, the PV is used to provide the electricity needed by the ASHP during the charging season and the surplus PV electricity is exported to the grid.

In Fig. 9, during the charging season, the borehole wall temperature in the dotted line changes according to the amount of heat flux injection. Because of the limited PV output, the heat flux from ASHP is only around 2,000W/m^3 during the charging season. With larger heat flux, the temperature increases fast and with lower heat flux, the temperature could decrease due to the heat dissipation to the surrounding ground. Overall, the borehole wall temperature still increases due to heat input. When the discharging season starts, the borehole temperature drops from 14°C to 11.7°C. During the charging season, the total heat flux injection from ASHP supported by the installed PV is 49,886W/m^3.

3) CASE 3 OPTIMIZED CHARGING STRATEGY

In the borehole inter-seasonal storage system, most heat loss appears during the charging season, so that it is significant to optimize the borehole charging. Cases 2 and 3 both require to charge the borehole during the charging season and Case 3 is carried out based on the data obtained from Case 2. By using the optimization method proposed in section IV, with the same total GSHP electricity consumption during the discharging season as in Case 2, the optimized heat flux injection is shown in Fig. 10 by the solid line. As shown, the ASHP starts charging the borehole arrays in the later time steps with the maximum available heat flux (4541W/m^3) output from the ASHP and before time step 16, ASHP is not operated.

To summarize, in these 3 cases, the heat demand during the discharging season is the same. The optimized charging strategy indicates that concentrated charging method leads to more efficient system performance than dispersed charging method as in Case 2. The solid line is the heat flux input which reaches the maximum level in the later stage of the charging season. With the maximum heat flux input, the borehole wall temperature (dotted line in Fig. 10) increases fast to a higher temperature level around 16°C, which

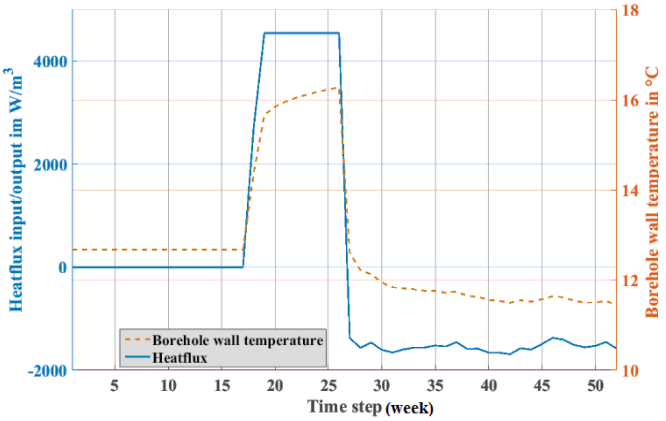

FIGURE. 10 Case 3 borehole wall temperature response to heat flux

provides the GSHP with an even higher temperature environment at the beginning of the discharging season.

C. RESULTS AND ANALYSIS

This section extensively compares the results of different charging strategies in terms of heat pump performances; total system operation cost and CO_2 emission compared to the traditional boiler.

1) HEAT FLUX WITH BOREHOLE TEMPERATURE

The charging strategies of cases 2 and 3 are compared in Fig. 11(a). In both cases, the borehole is charged during the charging season. Case 2 charges the borehole whenever there is free electricity provided by the installed PV (blue dotted line). Case 3 is the optimized charging strategy, i.e .a more concentrated charging (green solid line). In both cases, the GSHP consumes the same amount of electricity. However, during the charging season in Case 3, the total heat flux injection from ASHP is 39,028W/m^3, which is much lower than 49,886W/m^3 in Case 2.

In Case 2, with a limited amount of PV generation, ASHP provides lower heat flux between 1000 - 3000 W/m^3 in each time step. It is difficult to for the heat to cumulate and the heat loss is much higher in the whole charging season. In Case 3, the heat loss only occurs when the borehole starts charging. During the discharging season, the borehole temperature changes in a similar pattern as shown in Fig. 11(b) by the solid and dotted lines. Because of the active charging in the charging season, both cases 2 and 3 provide

GSHP higher temperature environment than base Case 1 in discharging season.

From Fig. 11(b), the temperature changes dramatically when charging or discharging starts. The reason for this dramatic change is that the U-shaped pipe carries high-temperature fluid, which is much higher than the ground temperature. When the temperature difference is big, the heat transfer is faster. When the heat settles down in the surrounding ground, due to the heat transfer parameters of different media, the temperature slowly reaches a steady state. As a result, the heat transfer happens faster in the beginning.

2) GSHP PERFORMANCE AND ELECTRICITY CONSUMPTION

Because of the active charging, cases 2 and 3 have higher borehole wall temperature Fig. 11(b), which affects the performance of GSHP in each time step during the discharging season. During the discharging season, the heat flux is extracted from the borehole and the borehole temperature is dropping constantly so that the CoP value is dropping during heating season Fig. 12(a). GSHP CoP

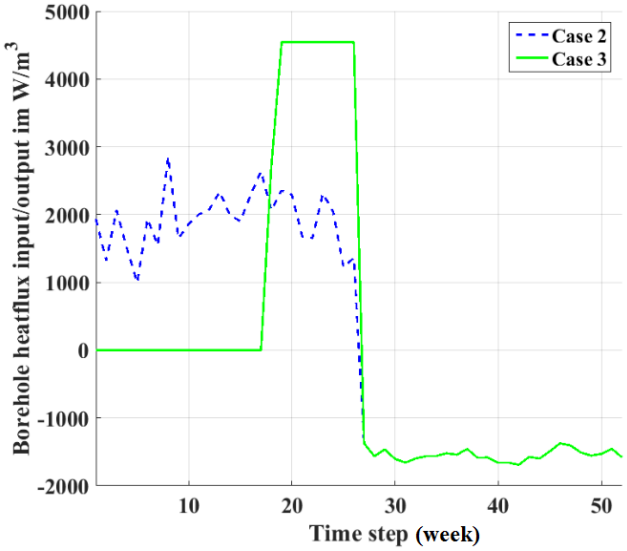

(a) Borehole charging strategy comparison between Case 2 and 3 (heat flux injection/extraction)

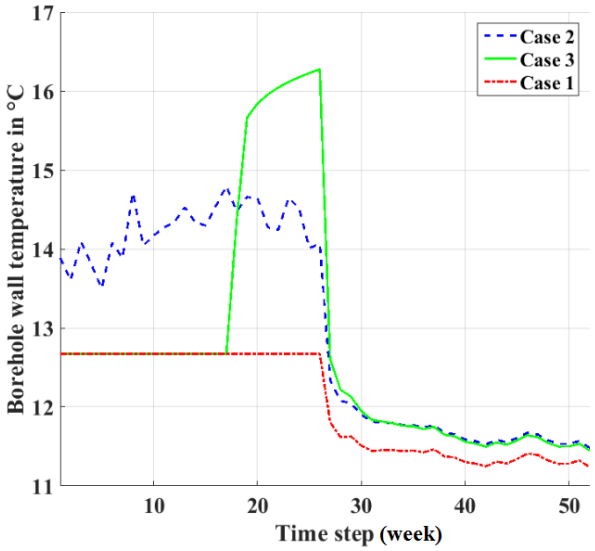

(b) Borehole wall temperatures changing pattern in Case 1, 2, and 3)

FIGURE. 11 Charging strategy and borehole wall temperature

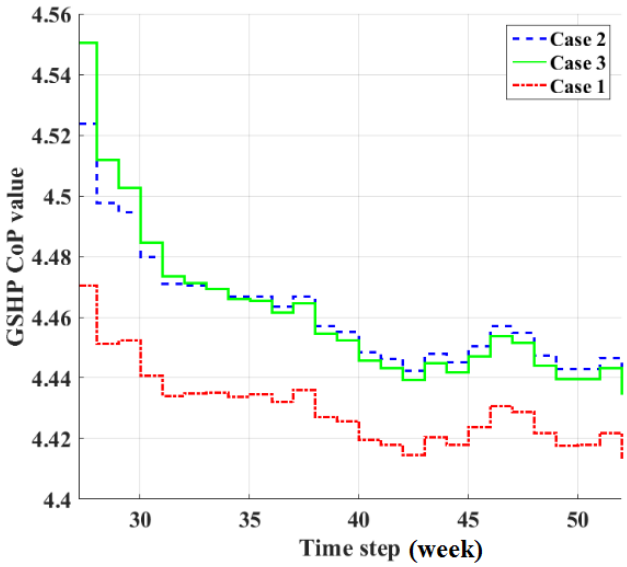

(a) Case 1, 2, and 3 GSHP CoP values comparison during the discharging season

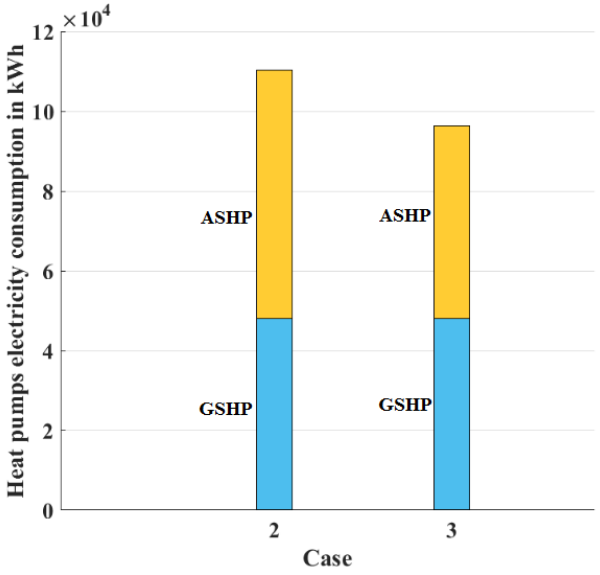

(b) Case 2 and 3 ASHP and GSHP electricity consumption comparison

FIGURE. 12 GSHP CoP comparison and ASHP electricity consumption comparison

values (between 4.56 to 4.44) in Cases 2 and 3 are shown in Fig. 12(a) compared to that in Case 1 (between 4.47 to 4.41) and in general, Case 2 and 3 have higher GSHP CoP value. As shown, Case 2 and Case 3 have slight difference GSHP CoP values due to the different charging strategies during the charging season, but the total electricity consumptions of GSHP in the discharging season are the same, which will be discussed later. Between the cases with active charging (Case 2 and 3) and with no-active charging (Case 1), the average borehole wall temperature and GSHP CoP values during the discharging season are around 0.31°C and 0.04 higher respectively according to the Fig.11(b) and 12(a).

TABLE III
DISCHARGING SEASON TOTAL ELECTRICITY CONSUMPTION

kWh	Case 1	Case 2 and 3
GSHP electricity consumption	48,448.52	48,107.64

Table III shows different GSHP electricity consumption in each case. In Case 1 and Case2 or 3, GSHP uses 48,448.52 kWh and 48,107.69 kWh electricity during the discharging season respectively. The electricity consumption is reduced by 340.88 kWh in Case 2 and 3 compared to Case 1.

3) ASHP PERFORMANCE AND ELECTRICITY CONSUMPTION

ASHP electricity consumption varies according to the charging strategies. Case 2 and Case 3 both charge the borehole during the charging season and the only difference is that in Case 3, the optimized charging strategy is applied.

In Fig. 12(b), the bottom part of the bars is the total GSHP electricity consumption during the discharging season in Case 2 and Case 3. The top parts of the bars are the electricity consumption of ASHP during the charging season. By adopting the optimized charging method, ASHP consumes 48,317kWh electricity in Case 3 which is 13,911kWh less than that in Case 2. The system uses less energy input to create the same heat output during the discharging season. As a result of the efficient electricity usage and effective borehole charging during the charging season, the electricity consumed by heat pumps (ASHP+GSHP) in the whole year is reduced by 12.61%.

4) TOTAL SYSTEM ELECTRICITY COST

This low carbon space heating system involves both PV and grid electricity and thus PV Feed-In-Tariff (FIT) and grid electricity price need to be considered in calculating costs. During the operation period, the import of electricity from the grid is needed when PV output is not sufficient to meet heat pump demand. Thus, the operation cost considered is due to buying electricity cost from the grid to meet heat pump minus the FIT earned by PV to export electricity to the grid. Maintenance cost is neglected as it is relatively low and this study is not performed under lifetime simulation.

$$C_{system} = (E_{HP} - E_{PV}) \times P_{grid} - FIT \times E_{exporting} \quad (10)$$

Where, C_{system} is system operation cost (£), E_{PV} is PV electricity for heat pump usage (kWh), E_{HP} is total electricity consumption of heat pump (kWh), $P_{grid\ electricty}$ is grid electricity price (£/kWh), E_{export} is PV output exported to the grid (kWh), and FIT is the unit benefit for PV to export extra electricity to the grid (£/kWh).

In Case 2, instead of exporting PV electricity to the grid, ASHP uses all the electricity generated by PV to charge the borehole. However, the injected heat flux is restrained by the PV generation so that the ASHP could not reach the maximum output heat flux the whole charging season.

In Case 3, the optimal charging strategy allows the PV to export electricity to the grid when the system decides not to charge the borehole during the charging season. The ASHP is supported by both the PV and grid to reach the maximum heat flux when it needs the system to charge. With the exported PV output, the total electricity cost actually decreases. The system costs in all three cases are shown in Fig. 13. The heating system in Cases 1 and 2 cost £2,572 and £2,524 respectively during the whole simulation time. In Case 3, the total cost is £2,014, decreasing by 21.69% and 20.19% compared to Cases 1 and 2.

5) CO_2 EMISSION

By comparing these 3 cases with the conventional heating system such as a boiler, the proposed borehole heating system CO_2 emission is reduced during the discharging season. Gas boiler CO_2 emission data is obtained from the British Gas website [27]. The total space heat demand is 214,591.77kWh. For the same amount of heat supplied by the boiler, 39,484.89 kg CO_2 is generated. By using the results from Table III and Fig. 5(a) of PV electricity generation, the CO_2 emission from the grid and PV during the discharging season is listed in Table IV. During the discharging season, Cases 1, 2 and 3 generate around 11,000 kg CO_2, reducing by around 70% compared to the case with pure boilers.

TABLE IV
CO_2 EMISSION IN DISCHARGING SEASON (kg)

CO_2 emission	*Case 1*	*Case 2 and 3*	*Boiler*
Grid plus PV	11,693.12	11,510.07	39,484.89

VI. CONCLUSION

This paper proposes a low carbon heating system by using borehole inter-seasonal heat storage and heat pumps to meet heating demand. A novel charging algorithm for the borehole system is developed. Through extensive demonstration, there are several key findings: i) borehole interseasonal thermal storage helps GSHP consume less electricity by charging it from PV; ii) the proposed borehole operation strategy enables the borehole to reach higher temperature with less heat loss and heat input, reducing the total operation cost via reducing the reliance on the grid electricity; iii) with less heat pump electricity consumption, this space heating system generates less CO_2 compared to the traditional boiler system. In addition, there are many important areas to be

considered in the future. Reducing the simulation time step can produce more accurate and detailed simulation results, informing real-time control. Besides, weather conditions considered in the operation of the system can add the uncertainties to both PV output and heating demand. In order to examine the impact of heat accumulation over the lifetime of the borehole storage system, the charging/discharging cycles should be further increased as well.

REFERENCES

[1] M. Li, P. Li, V. Chan, and A. C. K. Lai, "Full-scale temperature response function (G-function) for heat transfer by borehole ground heat exchangers (GHEs) from sub-hour to decades," *Applied Energy*, vol. 136, pp. 197-205, 12/31/ 2014.

[2] W. Wei, H. Da, and B. Simon Le, "Borehole active recharge benefit quantification on a community level low carbon heating system," in *2016 IEEE Power and Energy Society General Meeting (PESGM)*, 2016, pp. 1-5.

[3] E. I. S. Department for Business. (31 July 2013). *Domestic energy fact file and housing surveys*. Available: https://www.gov.uk/government/collections/domestic-energy-fact-file-and-housing-surveys

[4] R. Yao and K. Steemers, "A method of formulating energy load profile for domestic buildings in the UK," *Energy and Buildings*, vol. 37, pp. 663-671, 6// 2005.

[5] H. Meier and K. Rehdanz, "Determinants of residential space heating expenditures in Great Britain," *Energy Economics*, vol. 32, pp. 949-959, 2010/09/01/ 2010.

[6] T. Kanea, S. K. Firth, D. Allinson, K. N. Irvine, and K. J. Lomas. (05/2011). *Understanding occupant heating practices in UK dwellings*. Available: http://mmmm.lboro.ac.uk/doc/wrec%20paper%20-%20final%20submission.pdf

[7] S. H. Hong, T. Oreszczyn, and I. Ridley, "The impact of energy efficient refurbishment on the space heating fuel consumption in English dwellings," *Energy and Buildings*, vol. 38, pp. 1171-1181, 2006/10/01/ 2006.

[8] E. ICAX, the University of Bath, DECC. (2015, 10/04). *Owen Square Community Energy project*. Available: http://www.cepro.co.uk/2015/04/choices-solar-district-heat-study/

[9] E. N. A. Limited. (2017, 21/06/2017). *2050 Pathways for Domestic Heat*. Available: http://www.energynetworks.org/gas/futures/2050-pathways-for-domestic-heat.html

[10] M. Li and A. C. K. Lai, "Analytical model for short-time responses of ground heat exchangers with U-shaped tubes: Model development and validation," *Applied Energy*, vol. 104, pp. 510-516, 2013.

[11] M. Li and A. C. K. Lai, "New temperature response functions (G functions) for pile and borehole ground heat exchangers based on composite-medium line-source theory," *Energy*, vol. 38, pp. 255-263, 2012/02/01/ 2012.

[12] J. Claesson and S. Javed. (2011). *An analytical method to calculate borehole fluid temperatures for time-scales from minutes to decades*. Available: http://publications.lib.chalmers.se/records/fulltext/151315/local_151315.pdf

[13] M. Li and A. C. K. Lai, "Heat-source solutions to heat conduction in anisotropic media with application to pile and borehole ground heat exchangers," *Applied Energy*, vol. 96, pp. 451-458, 2012/08/01/ 2012.

[14] N. Diao, Q. Li, and Z. Fang, "Heat transfer in ground heat exchangers with groundwater advection," *International Journal of Thermal Sciences*, vol. 43, pp. 1203-1211, 2004/12/01/ 2004.

[15] N. Molina-Giraldo, P. Blum, K. Zhu, P. Bayer, and Z. Fang, "A moving finite line source model to simulate borehole heat exchangers with groundwater advection," *International Journal of Thermal Sciences*, vol. 50, pp. 2506-2513, 2011/12/01/ 2011.

[16] H. Zeng, N. Diao, and Z. Fang, "Heat transfer analysis of boreholes in vertical ground heat exchangers," *International Journal of Heat and Mass Transfer*, vol. 46, pp. 4467-4481, 2003/11/01/ 2003.

[17] A. Zarrella, M. Scarpa, and M. D. Carli, "Short time-step performances of coaxial and double U-tube borehole heat exchangers: Modeling and measurements," *HVAC&R Research*, vol. 17, pp. 959-976, 2011/12/01 2011.

[18] Y. Nam, R. Ooka, and S. Hwang, "Development of a numerical model to predict heat exchange rates for a ground-source heat pump system," *Energy and Buildings*, vol. 40, pp. 2133-2140, 2008/01/01/ 2008.

[19] H. Su, Q. Li, X. H. Li, Y. Zhang, Y. T. Kang, Z. H. Si, *et al.*, "Fast Simulation of a Vertical U-Tube Ground Heat Exchanger by Using a One-Dimensional Transient Numerical Model," *Numerical Heat Transfer, Part A: Applications*, vol. 60, pp. 328-346, 2011/08/15 2011.

[20] C. K. Lee, "Effects of multiple ground layers on thermal response test analysis and ground-source heat pump simulation," *Applied Energy*, vol. 88, pp. 4405-4410, 2011/12/01/ 2011.

[21] R. R. F. Al-Chalabi, "Thermal resistance of U-tube borehole heat exchanger system: numerical study," 2013.

[22] Y. Zhang, Y. Zhang, and P. Zhang, "Modeling and simulation of double-boreholes vertical U-shaped pipe heat transfer," ed, 2013, pp. 1978-1983.

[23] S. L. Weihua Yang, Xiaosong Zhang, "Numerical Simulation on Heat Transfer Characteristics of Soil Around U-Tube Underground Heat Exchangers," presented at the International Refrigeration and Air Conditioning Conference, 2008.

[24] F. De Ridder, M. Diehl, G. Mulder, J. Desmedt, and J. Van Bael, "An optimal control algorithm for borehole thermal energy storage systems," *Energy and Buildings*, vol. 43, pp. 2918-2925, 2011.

[25] I. f. E. Joint Researcg Centre, Renewable Energy Unit. *Photovoltaic Geographical Information System (PVGIS)*. Available: http://re.jrc.ec.europa.eu/pvgis/

[26] C. Gu, W. Yang, Y. Song, and F. Li, "Distribution Network Pricing for Uncertain Load Growth Using Fuzzy Set Theory," 2016.

[27] B. Gas. (2018). *Comparing your energy usage*. Available: http://www.britishgas.co.uk/help-and-advice/Online-account/Comparing-your-energy-usage/How-do-you-work-out-the-CO2-values.html